PHYSICAL REVIEW B **96**, 201103(R) (2017)

Realizing and adiabatically preparing bosonic integer and fractional quantum Hall states in optical lattices

Yin-Chen He,* Fabian Grusdt, Adam Kaufman, Markus Greiner, and Ashvin Vishwanath
Department of Physics, Harvard University, Cambridge, Massachusetts 02138, USA
(Received 3 April 2017; revised manuscript received 24 October 2017; published 3 November 2017)

We study the ground states of two-dimensional lattice bosons in an artificial gauge field. Using state-of-the-art density matrix renormalization group (DMRG) simulations we obtain the zero-temperature phase diagram for hard-core bosons at densities n_b with flux n_ϕ per unit cell, which determines a filling $\nu = n_b/n_\phi$. We find the bosonic Jain sequence [$\nu = p/(p+1)$] states, in particular, a bosonic integer quantum Hall phase at $\nu = 2$, are fairly robust in the hard-core boson limit, In addition to identifying Hamiltonians whose ground states realize these phases, we discuss their preparation, beginning from independent chains, and ramping up interchain couplings. Using time-dependent DMRG simulations, these are shown to reliably produce states close to the ground state for experimentally relevant system sizes. Our proposal only utilizes existing experimental capabilities.

DOI: 10.1103/PhysRevB.96.201103

The two-dimensional (2D) Bose-Hubbard model is one of the simplest many-body systems that exhibits nontrivial physics. Initially proposed as a model for the superconductor-insulator transition in solid state systems [1,2], it was later realized most cleanly in optical lattices of ultracold atoms [3,4]. It has been widely studied by varying the ratio of hopping to interaction strength t/U, and the filling n_b of bosons per site. A third natural parameter is the magnetic flux n_ϕ, the tuning of which has been demonstrated recently in ultracold atomic systems in periodically driven optical lattices [5]. The phase diagram as a function of magnetic flux through the unit cell is less understood. This is the bosonic analog of the Harper-Hofstadter problem of free electrons in a tight-binding model with magnetic flux [6]. However, to realize interesting phases, the bosonic problem is necessarily interacting (see also the related study of fermions [7–11]).

At finite flux density, quantum Hall phases (QHs) [12–14] of bosons might appear if the filling factor $\nu = n_b/n_\phi$ is appropriate. One interesting state corresponds to $\nu = 2$, which is called the bosonic integer quantum Hall state (BIQH) [15,16]. It belongs to the newly discovered symmetry protected topological (SPT) phase [17–19], different from all other fractional quantum Hall states that are intrinsically topologically ordered. This BIQH state was theoretically found before, e.g., two-component bosons or higher Chern number flatband model [20–27]. The BIQH indeed can be constructed using the well-known composite fermion approach [28]. Specifically, one can first attach one flux quantum to the bosons, converting them into composite fermions, and letting them form a $\nu_{\rm CF} = p$ integer quantum Hall state. This construction gives the so-called Jain sequence states at a filling factor $\nu = p/(p+1)$, and taking $p = -2$ gives the BIQH state [29].

For a given filling factor ν, there could be different competing phases (e.g., different QHs, ordered states). Which phase is the ground state is an energetic problem that usually differs case by case, but it is very useful if one can learn some general knowledge about the appearance of Jain's composite fermion states. For fermions, it is found that the Jain sequence state systematically appears in the lowest Landau level. However, bosons behave quite differently: Half of the Jain sequence (the hole part with $p < 0$) is missing in the continuum limit with the lowest Landau level of bosons ($U \ll t\phi$) (e.g., see a review in Ref. [30] for numerics and Refs. [31,32] for analytical results). Therefore, it is interesting to pass to the lattice, on which one can achieve the infinite interaction limit $U/t \to \infty$ that may not be continuously connected with the continuum limit. Indeed, early work motivating the search for lattice effects reported a candidate BIQH at low densities ($n = 1/7, 1/9$) [29]. Also, previous exact diagonalization (ED) calculations on small system sizes found several Jain's composite fermion states with $p = 1,2$ [29,33–35]. In this Rapid Communication, we systematically show that the full Jain sequence (at least up to $p = \pm 5$), in particular, the BIQH state, appears in the $U \to \infty$ limit.

Even if a quantum Hall state is the ground state of a simple Harper-Hofstadter model, it remains challenging for cold-atom experiments to realize. Cooling into a nontrivial ground state poses special challenges, particularly in the context of driven systems such as the Floquet engineered optical lattice systems [5,36–44]. We need a cooling scheme to overcome this issue. One way of cooling, called adiabatic preparation [45–49], begins with a trivial state with low entropy, which is then slowly ramped to the desired final state. Such adiabatic preparation schemes in general require a continuous phase transition between the initial state and the final state. For a quantum Hall state, an adiabatic preparation scheme is even more difficult, since usually an exotic phase transition, e.g., deconfined phase transition, will be involved [48]. Finding an appropriate adiabatic preparation scheme for optical lattice quantum Hall states is the second question on which we will make progress, and, in particular, our scheme appears to work for most quantum Hall phases, at least for the system sizes relevant for experiments.

We will first present our density matrix renormalization group (DMRG) simulation [50–52] which numerically finds robust Jain sequence states $p/(p+1)$ (e.g., $p = 1, \pm 2, \ldots, \pm 5$) on the lattice with a relatively high particle density. In particular, the BIQH state (at $p = -2$) is found robust with a short correlation length and quantized Hall

*Corresponding author: yinchenhe@g.harvard.edu

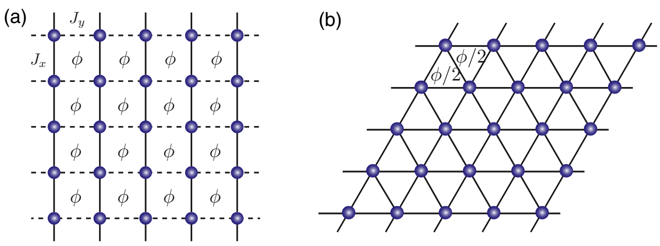

FIG. 1. Harper-Hofstadter model on (a) a square lattice with flux $\phi = 2\pi n_\phi$ on each square plaquette, and (b) a triangular lattice with flux $n_\phi/2$ on each triangle plaquette.

conductance. A related state was observed in the low-density limit in Ref. [29]. Next, we use time-dependent DMRG simulations [53–56] as well as exact diagonalization to discuss the adiabatic preparation scheme for quantum Hall phases, focusing on the BIQH state. The basic idea is beginning with the independent chain limit of one-dimensional (1D) Luttinger liquids, and ramping up interchain couplings that also introduce the flux. To benchmark the effectiveness of our preparation scheme, we utilize the wave-function overlap between the state generated by the time ramp and the true ground state as an indicator. We also discuss a physical diagnosis using a two-point correlation function to detect the gapless edge state of the quantum Hall phases.

Model and phases. We consider the Bose-Hubbard model (Harper-Hofstadter model) on a square (triangular) lattice (see Fig. 1),

$$H = -J\sum_{\langle ij\rangle} e^{iA_{ij}} a_i^\dagger a_j + U\sum_i n_i(n_i - 1). \tag{1}$$

The first term is the nearest-neighbor hopping subject to a background flux A_{ij}, with $\sum A = \phi = 2\pi n_\phi$ on each square plaquette (or $n_\phi/2$ on each triangle). The second term is the on-site Hubbard interactions, and we mainly consider the limit $U \to \infty$ that gives the hard-core boson constraint $n = 0,1$. Numerically, we confirm the phases also survive under finite U.

One may expect quantum Hall phases for a certain filling factor $\nu = n_b/n_\phi$, where n_b is the boson density per site. The simplest possibility is a Jain sequence with $\nu = p/(p+1) = n_b/n_\phi$ from the composite fermion approach [28]. First, one can attach one flux quantum to the boson, yielding the composite fermion. The composite fermions still have density n_b and see an effective flux $n_\phi - n_b = n_b/p$, then naturally they will form an integer quantum Hall state with $\nu_{\mathrm{CF}} = p$. Naively, the continuum limit, which can be formulated as the lowest Landau level with a contact Haldane's pseudopotential $V\delta(r - r')$, is the most ideal platform for quantum Hall phases. In that limit, however, several states, particularly the BIQH state ($p = -2$), were not found in the extensive study (e.g., see a review in Ref. [30]).

Here, we focus mainly on the limit with $U \to \infty$. Unexpectedly, we numerically find that the Jain sequence states ($p = 1, \pm 2, \ldots, \pm 5, \ldots$) systematically appear in this limit. We also note that even if $n_\phi \ll 1$, the system we consider here is still different from the continuum limit. It is because the infinite on-site interaction U will be much larger than the Landau level spacing ($\sim n_\phi J$), making the simple Landau level physics invalid. Theoretically, the flux attachment requires the boson to be a hard-core object, hence the infinite U may energetically help the flux attachment to happen. This may be an intrinsic mechanism for our numerical observation.

TABLE I. A brief summary of Jain's sequence on the square lattice with small $p = 1, \pm 2$ obtained in our DMRG simulations. n_b is the density per site. n_ϕ is the flux per square plaquette. The simulations are mainly carried on an infinite cylinder with circumference $L = 6, \ldots, 12$.

$\sigma^{xy} = \frac{p}{p+1}$	n_ϕ	n_b
	1/4	1/8
$p = 1$		
	1/5	1/10
$\sigma^{xy} = 1/2$	1/6	1/12
Laughlin state		
	...	...
	1/4	1/6
$p = 2$		
	1/5	2/15
$\sigma^{xy} = 2/3$		
	1/6	1/9
Halperin's (221) state		
	...	...
$p = -2$	1/6	1/3
$\sigma^{xy} = 2$	1/8	1/4
Bosonic integer	1/10	1/5
Quantum Hall	...	...

Several methods were applied to study this problem before [29,33–35,57–61]; here, we will use the infinite DMRG simulation [52] to tackle it. We numerically observe a Jain sequence states of bosons at filling factor $\nu = p/(p+1)$ for $p = 1, \pm 2, \ldots, \pm 5$. Generally, the instability of the Jain states grows with p. A consequence is that, to realize a larger p, one needs a more dilute density (meaning a smaller n_ϕ and n_b). On the other hand, we also find that the Jain sequence states are more stable on the triangular lattice [62]. Here and in the following, we mainly focus on small $p = 1, \pm 2$ on the square lattice as summarized in Table I. The results of larger p are summarized in the Supplemental Material [62]. We study an infinite cylinder with circumference $L_c = 6, \ldots, 12$ and different sizes give consistent results. For a smaller flux density n_ϕ than we show in Table I, we expect the same quantum Hall state still exists. A particularly interesting state corresponds to $p = -2$, that is, the BIQH state at $\nu = 2$. Unlike fractional QH, BIQH does not possess topological order, instead it is a SPT [protected by the $U(1)$ charge conservation]. So here our results provide a very simple setting for experimentally realizing the putative interacting SPT phase in spatial dimensions higher than $d = 1$.

We numerically diagnose those quantum Hall phases through their quantized Hall conductance (many-body Chern number). To measure the Hall conductance, we wrap the system on a cylinder, and measure the charge pumping by threading 2π flux [63,64]. The pumped charge is exactly the Hall conductance σ^{xy} [65]. As clearly shown in Fig. 2(a), the Hall conductance is precisely $\sigma^{xy} = 1/2,\ 2/3,\ 2$ for three

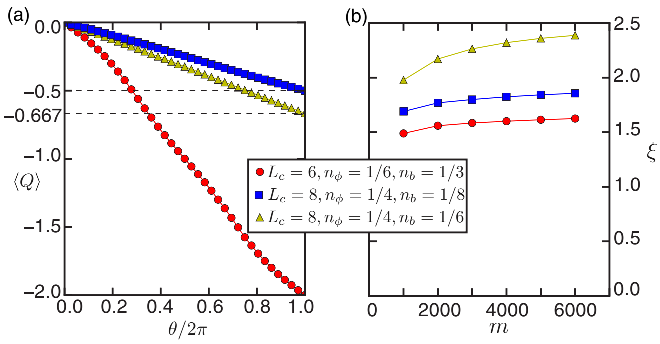

FIG. 2. Numerical diagnosis of quantum Hall states $\nu = 2$, 1/2, 2/3; L_c is the circumference. (a) Quantized Hall conductance measured from flux insertion on an infinite cylinder. Charge transfer as a function of flux: $\langle Q\rangle = -\sigma_{xy}\frac{\theta}{2\pi}$. (b) The correlation length ξ of the quantum Hall state vs bond dimension m in DMRG simulations showing convergence. The truncation error of DMRG simulation is around 10^{-8}–10^{-10}. The correlation length is small compared with the circumference, indicating that our DMRG simulation is reliably producing 2D physics.

quantum Hall states. Also, we find that the states have a short correlation length [Fig. 2(b)], indicating a fully gapped state.

Adiabatic preparation from the 1D phase. One important challenge for cold-atom experiments is to cool into the ground state. We now discuss one preparation scheme for preparing quantum Hall phases using adiabatic preparation starting from decoupled 1D wires. The idea is that we first turn off hopping along one direction (say, $J_y = 0$). In this limit, we get decoupled 1D Luttinger liquids with density n_b. Then we slowly turn on the hopping J_y (that also introduces the flux), which eventually yields a 2D bosonic quantum Hall phase at the isotropic limit $J_y = J_x$. The adiabatic preparation schemes by coupling smaller subsystems have also been used elsewhere [66].

Numerically, we find this scheme can achieve the adiabatic preparation for bosonic (both fractional and integer) quantum Hall phases. One piece of numerical evidence is the properties of the ground state as we ramp the system from 1D wires to a 2D quantum Hall state. First, we find the physical quantities (e.g., the energy and entanglement entropy) evolve continuously as we change the parameter (J_y). Second, we observe that the wave function of the ground state of the system is changing smoothly, namely, the wave-function overlap $|\langle\psi(J_y)|\psi(J_y+dJ_y)\rangle| \to 1$ as $dJ_y \to 0$.

To make a more direct contact with experiments, we also simulate the preparation scheme as the nonequilibrium process. It can be generally described by $|\psi_f\rangle = \int_0^T dt e^{-itH(t)}|\psi_0\rangle$. $H(t)$ is the time-dependent Hamiltonian that will be tuned experimentally,

$$H(t) = -J_x\sum_{\langle ij\rangle_x} e^{iA_{ij}}a_i^\dagger a_j - J_y(t)\sum_{\langle ij\rangle_y} e^{iA_{ij}}a_i^\dagger a_j + U\sum_i n_i(n_i-1), \quad (2)$$

with time-dependent hopping on the y direction, $J_y(t) = J_x t/T$. ψ_0 is the initial state, that is, the ground state of the starting Hamiltonian $H(0)$. Numerically, we first discretize the time-evolution operator $\int_0^T dt e^{-itH(t)} \approx \prod_{n=0}^m e^{-i(t_{n+1}-t_n)H(t_{n+1})}$, with $t_n = nT/m$, $m \gg 1$, and the final Hamiltonian $H(t_f = T)$ is the one in Eq. (1). Following the method introduced by Zaletel *et al.* [56], we then rewrite the operator $e^{-i(t_{n+1}-t_n)H(t_{n+1})}$ as a matrix product operator, and apply it to the wave function successively.

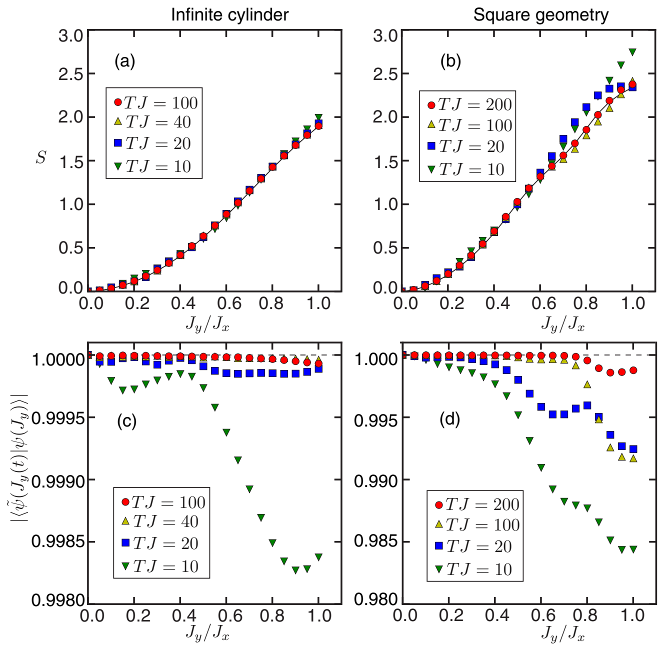

FIG. 3. Nonequilibrium dynamics simulation of the preparation scheme with different ramp times T, and we define $J = J_x$. We show the results of the BIQH state at $n_\phi = 1/6$, $n_b = 1/3$ of a square lattice placed on both the $L_c = 6$ infinite cylinder (a),(c) and the 6×6 square geometry (b),(d). (a),(b) show the time evolution of entanglement entropy, where the solid line represents the entanglement entropy of the ground state vs J_y/J_x, and the dots represent the entanglement entropy from the time evolution. (c),(d) shows the wave-function overlap per site between the ground state $\psi(J_y)$ and the state from time evolution $\tilde\psi[J_y(t)]$. Intriguingly, $TJ = 20$ seems to give a better ground state than $TJ = 100$; the physical reason is unclear.

Figure 3 shows the numerical results for the preparation scheme. We carry out simulations for (i) the infinite cylinder geometry (y direction is taken to infinite), and (ii) the finite square geometry that has an open boundary condition on both the x and y directions. To quantify how good the adiabatic preparation is, we compare the state from the time evolution ($\tilde\psi[J_y(t)]$) with the true ground state [$\psi(J_y)$] of the static Hamiltonian. Specifically, we compare the entanglement entropy and wave-function overlap between two states. Clearly, the adiabatic preparation works well for both schemes, and the quality of the adiabaticity increases as the preparation time becomes longer. In particular, the wave-function overlap (per site) can reach 0.9999, which is strong proof for our adiabatic preparation scheme.

The finite square geometry works worse than the infinite cylinder geometry [e.g., see Figs. 3(c) and 3(d)]. Such behavior is expected since the quantum Hall state on a finite square geometry has gapless edge modes. The gapless modes will

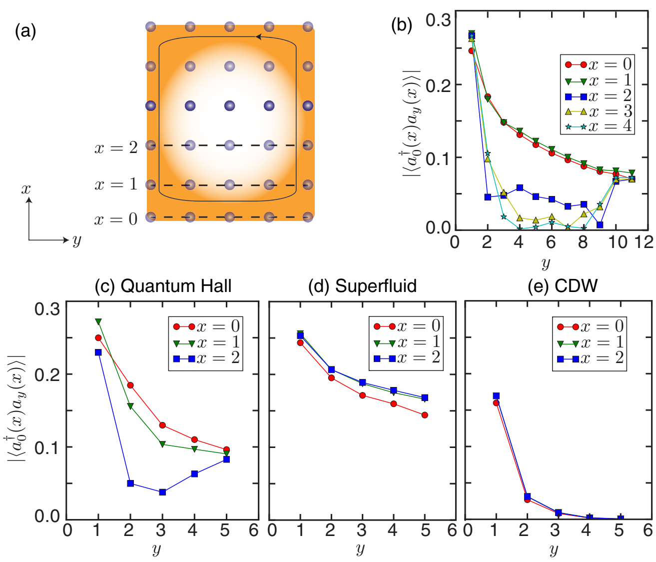

FIG. 4. Diagnosis of the quantum Hall state by measuring the two-point correlation function $|\langle a_0^\dagger(x)a_y(x)\rangle|$. (a) The cartoon picture for a quantum Hall state on a finite $L_x \times L_y$ cluster. For a quantum Hall state, $x = 0,1$ corresponds to the edge on which the correlation function decays algebraically. $x > 1$ corresponds to the bulk where the correlation function decays exponentially, however, if $a_y(x)$ hits the edge ($y \sim L_y$), the correlation function obeys the power law. Numerical results: (b) 9×12 cluster, $n_\phi = 1/6$, $n_b = 1/3$, $\nu = 2$ quantum Hall state. (c) 6×6, $n_\phi = 1/6$, $n_b = 1/3$, $\nu = 2$ quantum Hall state. (d) 6×6, $n_\phi = 0$, $n_b = 1/3$, superfluid. (e) 6×6, $n_\phi = 1/6$, $n_b = 1/2$, staggered potential $\Delta = 2$, charge density wave.

inevitably lead to some undesired excitations in an adiabatic preparation scheme. Fortunately, the experimental study as well as our numerical simulations are carried out on a finite system, which has a finite gap $\Delta E \propto 1/L$. Therefore, as long as the ramping time is long enough, the adiabatic preparation can be ideally achieved. The preparation scheme can be further optimized by adding a second tuning parameter, the magnetic flux $\phi = 2\pi n_\phi$ [47]. Tuning of ϕ has recently been realized using quantum gas microscopes [5]. More details can be found in the Supplemental Material [62].

Physical diagnosis of quantum Hall state. Finally, we study a simple correlation function based method to diagnose quantum Hall states in mesoscopic geometries. Although it is presently unclear how to directly measure this quantity in experiments, this will serve as a proxy for other correlation function based approaches to study quantum Hall states. The QH state has a gapped bulk but a gapless edge. To observe this property, one can measure the correlation function $\langle a_0^\dagger(x)a_y(x)\rangle$ along one direction, as shown in Fig. 4(a). x represents the position on the $\vec{x}$ direction, and $a_0(x)$ is always placed on the edge. When $x \sim 0$, the two-point correlation function is always measured on the edge, and hence will give a power law decaying behavior $\langle a_0^\dagger(x)a_y(x)\rangle \propto 1/y^\alpha$. On the other hand, when x is placed in the middle of the sample ($x \sim L_x/2$), $\langle a_0^\dagger(x)a_y(x)\rangle$ is measuring the correlation function in the bulk, yielding an exponentially decay behavior $e^{-y/\xi}$. However, once $a_r(x)$ hits the edge ($r \sim L_y$), $\langle a_0^\dagger(x)a_y(x)\rangle$ will follow a power law decay again. In summary, the two-point correlation functions behave as (we consider $x \leqslant L_x/2$ due to the symmetry),

$$\langle a_0^\dagger(x)a_y(x)\rangle \propto \begin{cases} 1/y^\alpha, & x \sim 0, \\ e^{-y/\xi}, & x \sim L_x/2, y < L_y, \\ 1/(y+2x)^\alpha, & x \sim L_x/2, y \sim L_y. \end{cases} \quad (3)$$

Figure 4(b) shows the data of two-point correlation functions of the bosonic integer quantum Hall state on a large system, 9×12 cluster (from DMRG). It is consistent with the above scaling behavior, Eq. (3). In particular, when $x \sim L_x/2$, the correlation function shows a nonmonotonic behavior: At first it decays fast, but then suddenly increases as a_y hits the edge. Such scaling behavior is also visible on a small system size, e.g., 6×6 cluster in Fig. 4(c). In contrast, a superfluid [Fig. 4(d)] and a charge density wave [Fig. 4(e)] do not show any nonmonotonic behavior. The state from our adiabatic preparation protocol also admits such nonmonotonic correlations (see Supplemental Material [62]), demonstrating that it retains physical characteristics of the ground state.

Conclusion and outlook. We study quantum Hall phases and their adiabatic preparation scheme in the Harper-Hofstadter model with hard-core bosons. Our theoretical study lends support to Jain's composite fermion picture in a regime where lattice effects play an important role. We note a recent work finds another setting for Jain's composite fermion states of bosons [67]. On the other hand, our work indicates a way forward for the experimental study of quantum Hall phases in optical lattices. It is interesting to understand the nature of the phase transition from the 1D wires to 2D quantum Hall phases. Another interesting problem is to come up with experimental measurement protocols, such as measuring the Hall conductance [38] or detecting the edge state (e.g., Refs. [68,69]).

Acknowledgments. We acknowledge stimulating discussions with Eugene Demler, Frank Pollmann, Chong Wang, Norman Yao, and Liujun Zou. Y.-C.H. thanks F. Pollmann for sharing the TENPY package to do the simulations of time-dependent DMRG, and thanks N. Yao for sharing unpublished ED results. Y.-C.H. and F.G. are supported by a postdoctoral fellowship from the Gordon and Betty Moore Foundation, under the EPiQS initiative, GBMF4306, at Harvard University. A.V. is supported by a Simons Investigator Award and by the AFOSR MURI Grant No. FA9550- 14-1-0035.

[1] M. P. A. Fisher, P. B. Weichman, G. Grinstein, and D. S. Fisher, Boson localization and the superfluid-insulator transition, Phys. Rev. B **40**, 546 (1989).

[2] S. L. Sondhi, S. M. Girvin, J. P. Carini, and D. Shahar, Continuous quantum phase transitions, Rev. Mod. Phys. **69**, 315 (1997).

[3] M. Greiner, O. Mandel, T. Esslinger, T. W Hänsch, and I. Bloch, Quantum phase transition from a superfluid to a Mott insulator in a gas of ultracold atoms, Nature (London) **415**, 39 (2002).

[4] X. Zhang, C.-L. Hung, S.-K. Tung, and C. Chin, Observation of quantum criticality with ultracold atoms in optical lattices, Science **335**, 1070 (2012).

[5] M. E. Tai, A. Lukin, M. Rispoli, R. Schittko, T. Menke, D. Borgnia, P. M. Preiss, F. Grusdt, A. M. Kaufman, and M. Greiner, Microscopy of the interacting Harper-Hofstadter model in the two-body limit, Nature (London) **546**, 519 (2017).

[6] D. R. Hofstadter, Energy levels and wave functions of Bloch electrons in rational and irrational magnetic fields, Phys. Rev. B **14**, 2239 (1976).

[7] T. Neupert, L. Santos, C. Chamon, and C. Mudry, Fractional Quantum Hall States at Zero Magnetic Field, Phys. Rev. Lett. **106**, 236804 (2011).

[8] N. Regnault and B. A. Bernevig, Fractional Chern Insulator, Phys. Rev. X **1**, 021014 (2011).

[9] E. Tang, J.-W. Mei, and X.-G. Wen, High-Temperature Fractional Quantum Hall States, Phys. Rev. Lett. **106**, 236802 (2011).

[10] D. Sheng, Z.-C. Gu, K. Sun, and L. Sheng, Fractional quantum Hall effect in the absence of Landau levels, Nat. Commun. **2**, 389 (2011).

[11] A. G. Grushin, Á. Gómez-León, and T. Neupert, Floquet Fractional Chern Insulators, Phys. Rev. Lett. **112**, 156801 (2014).

[12] K. V. Klitzing, G. Dorda, and M. Pepper, New Method for High-Accuracy Determination of the Fine-Structure Constant Based on Quantized Hall Resistance, Phys. Rev. Lett. **45**, 494 (1980).

[13] D. C. Tsui, H. L. Stormer, and A. C. Gossard, Two-Dimensional Magnetotransport in the Extreme Quantum Limit, Phys. Rev. Lett. **48**, 1559 (1982).

[14] R. B. Laughlin, Anomalous Quantum Hall Effect: An Incompressible Quantum Fluid with Fractionally Charged Excitations, Phys. Rev. Lett. **50**, 1395 (1983).

[15] Y.-M. Lu and A. Vishwanath, Theory and classification of interacting integer topological phases in two dimensions: A Chern-Simons approach, Phys. Rev. B **86**, 125119 (2012).

[16] T. Senthil and M. Levin, Integer Quantum Hall Effect for Bosons, Phys. Rev. Lett. **110**, 046801 (2013).

[17] X. Chen, Z.-C. Gu, Z.-X. Liu, and X.-G. Wen, Symmetry protected topological orders and the group cohomology of their symmetry group, Phys. Rev. B **87**, 155114 (2013).

[18] F. D. M. Haldane, Nonlinear Field Theory of Large-Spin Heisenberg Antiferromagnets: Semiclassically Quantized Solitons of the One-Dimensional Easy-Axis Néel State, Phys. Rev. Lett. **50**, 1153 (1983).

[19] F. Pollmann, A. M. Turner, E. Berg, and M. Oshikawa, Entanglement spectrum of a topological phase in one dimension, Phys. Rev. B **81**, 064439 (2010).

[20] S. Furukawa and M. Ueda, Integer Quantum Hall State in Two-Component Bose Gases in a Synthetic Magnetic Field, Phys. Rev. Lett. **111**, 090401 (2013).

[21] S. D. Geraedts and O. I. Motrunich, Exact realization of integer and fractional quantum Hall phases in $u(1) \times u(1)$ models in $(2+1)$D, Ann. Phys. **334**, 288 (2013).

[22] N. Regnault and T. Senthil, Microscopic model for the boson integer quantum Hall effect, Phys. Rev. B **88**, 161106 (2013).

[23] Y.-H. Wu and J. K. Jain, Quantum Hall effect of two-component bosons at fractional and integral fillings, Phys. Rev. B **87**, 245123 (2013).

[24] A. Sterdyniak, N. R. Cooper, and N. Regnault, Bosonic Integer Quantum Hall Effect in Optical Flux Lattices, Phys. Rev. Lett. **115**, 116802 (2015).

[25] Y.-C. He, S. Bhattacharjee, R. Moessner, and F. Pollmann, Bosonic Integer Quantum Hall Effect in an Interacting Lattice Model, Phys. Rev. Lett. **115**, 116803 (2015).

[26] G. Möller and N. R. Cooper, Fractional Chern Insulators in Harper-Hofstadter Bands with Higher Chern Number, Phys. Rev. Lett. **115**, 126401 (2015).

[27] T.-S. Zeng, W. Zhu, and D. N. Sheng, Bosonic integer quantum Hall states in topological bands with Chern number two, Phys. Rev. B **93**, 195121 (2016).

[28] J. K. Jain, Composite-Fermion Approach for the Fractional Quantum Hall Effect, Phys. Rev. Lett. **63**, 199 (1989).

[29] G. Möller and N. R. Cooper, Composite Fermion Theory for Bosonic Quantum Hall States on Lattices, Phys. Rev. Lett. **103**, 105303 (2009).

[30] N. R. Cooper, Rapidly rotating atomic gases, Adv. Phys. **57**, 539 (2008).

[31] F. Harper, S. H. Simon, and R. Roy, Perturbative approach to flat Chern bands in the Hofstadter model, Phys. Rev. B **90**, 075104 (2014).

[32] T. Scaffidi and S. H. Simon, Exact solutions of fractional Chern insulators: Interacting particles in the Hofstadter model at finite size, Phys. Rev. B **90**, 115132 (2014).

[33] A. S. Sørensen, E. Demler, and M. D. Lukin, Fractional Quantum Hall States of Atoms in Optical Lattices, Phys. Rev. Lett. **94**, 086803 (2005).

[34] R. N. Palmer, A. Klein, and D. Jaksch, Optical lattice quantum Hall effect, Phys. Rev. A **78**, 013609 (2008).

[35] M. Hafezi, A. S. Sørensen, E. Demler, and M. D. Lukin, Fractional quantum Hall effect in optical lattices, Phys. Rev. A **76**, 023613 (2007).

[36] M. Aidelsburger, M. Atala, M. Lohse, J. T. Barreiro, B. Paredes, and I. Bloch, Realization of the Hofstadter Hamiltonian with Ultracold Atoms in Optical Lattices, Phys. Rev. Lett. **111**, 185301 (2013).

[37] M. Atala, M. Aidelsburger, M. Lohse, J. T Barreiro, B. Paredes, and I. Bloch, Observation of chiral currents with ultracold atoms in bosonic ladders, Nat. Phys. **10**, 588 (2014).

[38] M. Aidelsburger, M. Lohse, C. Schweizer, M. Atala, J. T. Barreiro, S. Nascimbene, N. R. Cooper, I. Bloch, and N. Goldman, Measuring the Chern number of Hofstadter bands with ultracold bosonic atoms, Nat. Phys. **11**, 162 (2015).

[39] D. Jaksch and P. Zoller, Creation of effective magnetic fields in optical lattices: The Hofstadter butterfly for cold neutral atoms, New J. Phys. **5**, 56 (2003).

[40] J. Dalibard, F. Gerbier, G. Juzeliūnas, and P. Öhberg, Colloquium: Artificial gauge potentials for neutral atoms, Rev. Mod. Phys. **83**, 1523 (2011).

[41] N. R. Cooper, Optical Flux Lattices for Ultracold Atomic Gases, Phys. Rev. Lett. **106**, 175301 (2011).

[42] F. Gerbier and J. Dalibard, Gauge fields for ultracold atoms in optical superlattices, New J. Phys. **12**, 033007 (2010).

[43] A. R. Kolovsky, Creating artificial magnetic fields for cold atoms by photon-assisted tunneling, Europhys. Lett. **93**, 20003 (2011).

[44] N. Goldman, G. Juzeliūnas, P. Öhberg, and I. B. Spielman, Light-induced gauge fields for ultracold atoms, Rep. Prog. Phys. **77**, 126401 (2014).

[45] A. S. Sørensen, E. Altman, M. Gullans, J. V. Porto, M. D. Lukin, and E. Demler, Adiabatic preparation of many-body states in optical lattices, Phys. Rev. A **81**, 061603 (2010).

[46] M. Popp, B. Paredes, and J. I. Cirac, Adiabatic path to fractional quantum Hall states of a few bosonic atoms, Phys. Rev. A **70**, 053612 (2004).
[47] F. Grusdt, F. Letscher, M. Hafezi, and M. Fleischhauer, Topological Growing of Laughlin States in Synthetic Gauge Fields, Phys. Rev. Lett. **113**, 155301 (2014).
[48] M. Barkeshli, N. Y. Yao, and C. R. Laumann, Continuous Preparation of a Fractional Chern Insulator, Phys. Rev. Lett. **115**, 026802 (2015).
[49] E. Kapit, M. Hafezi, and S. H. Simon, Induced Self-Stabilization in Fractional Quantum Hall States of Light, Phys. Rev. X **4**, 031039 (2014).
[50] S. R. White, Density Matrix Formulation for Quantum Renormalization Groups, Phys. Rev. Lett. **69**, 2863 (1992).
[51] S. R. White, Density-matrix algorithms for quantum renormalization groups, Phys. Rev. B **48**, 10345 (1993).
[52] I. P. McCulloch, Infinite size density matrix renormalization group, revisited, arXiv:0804.2509.
[53] G. Vidal, Efficient Classical Simulation of Slightly Entangled Quantum Computations, Phys. Rev. Lett. **91**, 147902 (2003).
[54] S. R. White and A. E. Feiguin, Real-Time Evolution Using the Density Matrix Renormalization Group, Phys. Rev. Lett. **93**, 076401 (2004).
[55] A. J. Daley, C. Kollath, U. Schollwöck, and G. Vidal, Time-dependent density-matrix renormalization-group using adaptive effective Hilbert spaces, J. Stat. Mech.: Theory Exp. (2004) P04005.
[56] M. P. Zaletel, R. S. K. Mong, C. Karrasch, J. E. Moore, and F. Pollmann, Time-evolving a matrix product state with long-ranged interactions, Phys. Rev. B **91**, 165112 (2015).
[57] R. N. Palmer and D. Jaksch, High-Field Fractional Quantum Hall Effect in Optical Lattices, Phys. Rev. Lett. **96**, 180407 (2006).
[58] A. Sterdyniak, N. Regnault, and G. Möller, Particle entanglement spectra for quantum Hall states on lattices, Phys. Rev. B **86**, 165314 (2012).
[59] A. Sterdyniak, B. A. Bernevig, N. R. Cooper, and N. Regnault, Interacting bosons in topological optical flux lattices, Phys. Rev. B **91**, 035115 (2015).
[60] S. S. Natu, E. J. Mueller, and S. Das Sarma, Competing ground states of strongly correlated bosons in the Harper-Hofstadter-Mott model, Phys. Rev. A **93**, 063610 (2016).
[61] D. Hügel, H. U. R. Strand, P. Werner, and L. Pollet, Anisotropic Harper-Hofstadter-Mott model: Competition between condensation and magnetic fields, Phys. Rev. B **96**, 054431 (2017).
[62] See Supplemental Material at http://link.aps.org/supplemental/10.1103/PhysRevB.96.201103 for additional numerical data.
[63] Y.-C. He, D. N. Sheng, and Y. Chen, Obtaining topological degenerate ground states by the density matrix renormalization group, Phys. Rev. B **89**, 075110 (2014).
[64] A. G. Grushin, J. Motruk, M. P. Zaletel, and F. Pollmann, Characterization and stability of a fermionic $\nu = 1/3$ fractional Chern insulator, Phys. Rev. B **91**, 035136 (2015).
[65] R. B. Laughlin, Quantized Hall conductivity in two dimensions, Phys. Rev. B **23**, 5632 (1981).
[66] A. M. Rey, R. Sensarma, S. Fölling, M. Greiner, E. Demler, and M. D. Lukin, Controlled preparation and detection of d-wave superfluidity in two-dimensional optical superlattices, Europhys. Lett. **87**, 60001 (2009).
[67] S. D. Geraedts, C. Repellin, C. Wang, R. S. K. Mong, T. Senthil, and N. Regnault, Emergent particle-hole symmetry in spinful bosonic quantum Hall systems, Phys. Rev. B **96**, 075148 (2017).
[68] S. Yin and B. Béri, Universality and quantized response in bosonic mesoscopic tunneling, Phys. Rev. B **93**, 245142 (2016).
[69] X.-Y. Dong, A. G. Grushin, J. Motruk, and F. Pollmann, Edge state dynamics in bosonic fractional Chern insulators, arXiv:1710.03756 .